

## Adsorption of Commercial Dyes using Chemically Modified Biochars Derived from Empty Fruit Bunches

Sarmila Gunasekaran, Samsuri Abd Wahid\*, Halmi Mohd Izuan Effendi

Department of Land Management, Faculty of Agriculture, Universiti Putra Malaysia, Serdang, Malaysia

\*Corresponding author (e-mail: samsuriaw@upm.edu.my)

In this study, the adsorption capacities of activated empty fruit bunch biochar (EFBB) (an oil palm industry byproduct that is converted into biochar) for methylene blue (MB) and direct red 80 (DR 80) commercial dyes were evaluated. The EFBB was chemically modified by treating it with sulphuric acid ( $\text{H}_2\text{SO}_4$ ), potassium hydroxide (KOH) or iron chloride ( $\text{FeCl}_3$ ) to produce acid-treated biochar (A-EFBB), alkali-treated biochar (B-EFBB) and iron-coated biochar (Fe-EFBB). The characteristics of EFBB, chemically modified EFBB and activated carbon (AC) were determined. These adsorbents were used to remove the cationic MB and anionic DR 80 dyes at different initial concentrations and their adsorption capacities were compared. The Langmuir model fitted the isotherm data better than Freundlich's model, which indicated that adsorption was homogeneous and monolayer. Results for MB showed that the adsorption capacity was in the order: A-EFBB (125 mg/g) > B-EFBB (76.34 mg/g) > Fe-EFBB (10.13 mg/g) > EFBB (6.14 mg/g). For DR 80, the results showed that the adsorption capacity was in the order: B-EFBB (78.13 mg/g) > A-EFBB (40.16 mg/g) > Fe-EFBB (4.71 mg/g) > EFBB (1.15 mg/g).

**Key words:** Adsorption; dyes; biochar; chemical activation; oil palm

*Received: October 2021; Accepted: January 2022*

Water pollution is a serious problem in developing countries like Malaysia and this issue impacts the sustainability of water resources. It also affects living plants and organisms as well as population health and the economy [1]. Notably, in 2017, foreign and domestic investment in Malaysia's textile industry earned a total revenue of RM 428.8 million [2]. While having a huge effect on the economy, the textile industry uses an enormous amount of water for its preparation and dyeing processes. Consequently, it consumes up to 3000 m<sup>3</sup> of water a day and accounts for 22% of the total volume of industrial wastewater produced in Malaysia [3, 4]. Industries involving dyes are rapidly growing in Malaysia and synthetic dyes are widely used in the textile, paper, leather, pharmaceutical and printing industries [5-7], but dye effluents are released directly into the environment and cause water pollution [4]. Even the smallest amount of dye in a sample of water can make it unsuitable for human consumption. Dyes also reduce sunlight penetration in water and so inhibit the growth of aquatic plants. Aside from being toxic to aquatic life, dyes may also be mutagenic, carcinogenic and cause severe damage to the human body such as dysfunction of the kidneys, reproductive system, liver, brain and central nervous system [8, 9, 5]. Thus, wastewater polluted with dyes needs to be properly treated before it can be released into the environment.

Methylene blue (MB) and Direct Red 80 (DR 80) dyes are among the hazardous materials found in textile

effluent [10]. MB is a cationic dye commonly used for dyeing cotton, wool, and silk. Some of the severe symptoms caused by MB include eye burns in humans and animals, methemoglobinemia, cyanosis, convulsions, tachycardia, dyspnea, irritation to the skin, and if ingested, irritation to the gastrointestinal tract, nausea, vomiting, and diarrhoea [11]. DR 80 is an anionic azo dye, one of the largest classes of dyes used in industry, which is often used for dyeing textiles and leather [12, 13]. These contain one or more azo bonds ( $-\text{N}=\text{N}-$ ) and aromatic rings, which are considered toxic and mutagenic to living organisms. Typically, the acute toxicity of an azo dye is low, but it may cause skin and eye irritation, weakness and dizziness [13, 14].

A variety of methods have been developed for the treatment of dye-bearing wastewater such as coagulation, flocculation, oxidation, biological treatments, membrane filtration and adsorption. Yet some of these techniques have major drawbacks such as cost and time [9, 15]. Among these methods, adsorption shows a number of essential benefits such as flexibility and simplicity of the technique, ease of operation and insensitivity to toxic substances. Thus, adsorption is preferable over other methods and is widely used because of its low cost and high efficiency. Recently, the use of adsorbents prepared from agricultural by-products such as biochar has been thoroughly investigated due to its cost effectiveness and high adsorption capacities [16]. Biochar is a carbonaceous

material obtained from the pyrolysis of biomass under zero or limited oxygen conditions and at a relatively low temperature, usually below 700°C. It has been recognized as a good sorbent for different kinds of organic and inorganic pollutants [17, 18]. However, biochar usually possesses a lower adsorption capacity compared to activated carbon. Therefore, biochar has to be activated to increase its surface area, porosity and surface functional groups, which consequently enhances its adsorption capacity [19, 20].

Oil palm empty fruit bunches are a major agricultural waste generated by the oil palm industry. These can be converted to biochar, which are good adsorbents for the removal of dyes from aqueous solutions [21]. In this study, empty fruit bunch biochar (EFBB) was chemically modified and its respective adsorption capacities for MB and DR 80 were evaluated. The adsorption capacities of these chemically modified biochars were compared with those of non-modified biochar as well as to an activated carbon (AC).

## MATERIALS AND METHODS

### 1. Chemicals and Materials

All chemical used were of analytical grade. Ultrapure water (electrical resistivity 18.2 MΩ cm<sup>-1</sup>) was used to prepare all solutions throughout this study. Sodium hydroxide (NaOH), potassium hydroxide (KOH), hydrochloric acid (HCl) and sulphuric acid (H<sub>2</sub>SO<sub>4</sub>) were purchased from R&M Chemicals while Methylene Blue (MB) and Direct Red 80 (DR 80) dyes were purchased from Sigma-Aldrich. pH solutions were adjusted using either 1 M sodium hydroxide (NaOH) or 1 M hydrochloric acid (HCl). Empty fruit bunch biochar (EFBB) was purchased from the Malaysian Palm Oil Board (MPOB) station, located at Pekan Bangi Lama, Malaysia. The biochar was brought to the laboratory, where it was ground and passed through a 250 µm metal sieve (Laboratory Test Sieve Endecotts Ltd., UK). Meanwhile, activated carbon produced from acid-washed lignite carbon with a particle size of 12-20 mesh was purchased from Sigma-Aldrich (Darco®).

### 2. Chemical Modification of Biochar

Chemically modified biochars were prepared by following the methods prescribed by both Liu et al. (2012) [6] and Sajab et al. (2013) [22]. 20 g of EFBB crude biochar was placed in a flask to which was added 200 mL of either 10 % H<sub>2</sub>SO<sub>4</sub> (v/v) or 3 M KOH solution and the solution was stirred using a magnetic stirrer for 1 hour at 60 – 70 °C. Then, the biochar was rinsed with deionized water until the pH of the washed liquid was around 7.0. The wet biochars were dried at 80 °C for 12 h and then stored in desiccators for later use. The biochars prepared from the acid and base were

designated as A-EFBB and B-EFBB, respectively.

### 3. Iron Impregnation of Biochar

Surface modification of the EFBB was done by coating the biochar with FeCl<sub>3</sub> according to the procedure described by Huang et al. (2017) [23]. The optimum equilibrium time and the concentration of the biochar were determined prior to the coating procedure. 5 g of EFBB was impregnated in a 1 L solution containing 1000 mg/L of Fe (III) prepared using FeCl<sub>3</sub> salt. The solution pH was adjusted to 6 using either 1 M HCl or 1 M NaOH. The mixture of biochar and Fe (III) solution was shaken for 24 h and the biochar was washed with deionized water several times until free Fe was no longer detected in the filtrate. The Fe coated biochar was then filtered on Whatman No. 42 filter paper and oven dried at 105°C for 24 hours. The EFBB was then washed several times with deionized water and dried for 48 h in an oven at 50 °C. The biochar prepared via this treatment was designated as Fe-EFBB.

### 4. Characterisation of EFBB, Chemically Modified EFBB and Activated Carbon

The pH values of EFBB, Fe-EFBB, A-EFBB, B- EFBB and AC were measured in a 4:100 (w/v) suspension of adsorbents in water using a pH meter (Model Metrohm® 827, USA) as described by Samsuri et al. (2013) [24]. The EC reading was measured according to Savova et al. (2001) [25] by soaking the adsorbent in deionized water at a solid to water ratio of 1:5 (w/v) and agitated for 24 h. The reading was measured using a CON 700 EC meter (Eutech Instruments, USA). The exchangeable bases of adsorbents were extracted with ammonium acetate and measured using a Perkin Elmer AAnalyst 400 Atomic Absorption Spectrometer (AAS) [25].

The ash content of the biochars and AC was determined by dry combustion. 5.0 g of adsorbent was heated at 500 °C for 8 h [26]. The crucible was then cooled to room temperature and reweighed. The ash content was calculated as:

$$\text{Ash content} = \frac{\text{weight of ash (g)}}{\text{dry mass of adsorbent (g)}} \times 100\% \quad (1)$$

The acidic groups on the surface of the adsorbents were determined by the Boehm titration method [27]. The number of acidic sites was determined based on three assumptions: (i) that NaOH neutralizes carboxylic, lactonic, and phenolic groups; (ii) that Na<sub>2</sub>CO<sub>3</sub> neutralizes carboxylic and lactonic groups; and (iii) that NaHCO<sub>3</sub> neutralizes only carboxylic groups [28]. The total carbon, hydrogen, nitrogen and sulphur content in the adsorbents were determined using a LECO TruSpec CHNS analyser.

The surface area of the adsorbents was measured with N<sub>2</sub> adsorption at 77.3 K, using a surface area analyzer (Autosorb-1, Quantochrome Instruments, USA). Prior to N<sub>2</sub> adsorption, the adsorbent sample was degassed at 200 °C for 9 h. The multipoint Brunauer–Emmett–Teller (BET) method was employed to calculate total surface area. The pore volume was calculated from their desorption isotherms using the Barrett–Joyner–Halenda (BJH) method [23, 25, 22]. The presence of surface functional groups in the adsorbent was determined using a Spectrum 100 Perkin-Elmer FTIR spectrometer with a resolution of 4 cm<sup>-1</sup> operating in the range of 300–4000 cm<sup>-1</sup>. The zeta potential of the adsorbents was measured using a Malvern® Zetasizer Nano instrument according to the method of Salame and Bandosz (2001) [29].

The surface morphology analyses of the adsorbents were conducted using a scanning electron microscope (JEOL JSM-IT 100, Japan) while the ASTM D4607-94 (1999) procedure was used to estimate the iodine number of each adsorbent. The iodine number was calculated using the following equation:

$$\frac{X}{M} = \frac{A - BS}{M} \quad (2)$$

where, X/M is the amount of iodine adsorbed per gram of adsorbent (mg/g), A is N<sub>2</sub> (12693.0), N<sub>2</sub> is the normality of iodine, S is the volume of sodium thiosulfate, mL, M is mass of carbon (g), B is N<sub>1</sub>\* 126.93 and N<sub>1</sub> is normality of sodium thiosulfate.

## 5. Batch Equilibrium Adsorption Study

A batch adsorption experiment was carried out to determine and compare the adsorption capacities of EFBB, chemically modified EFBB and AC for MB and DR 80 dyes at various initial concentrations. Stock solutions of MB (1000 mg/L) and DR 80 (1500 mg/L) were prepared. The experiment was carried out at room temperature (25 ± 1.5 °C) using approximately 0.5 g of adsorbent in centrifuge tubes containing 40 mL of either MB or DR 80 dyes, at a range of concentrations from 5–450 mg/L. The optimum equilibrium time and adsorbent to solution ratio for the batch equilibrium method were predetermined at 24 h and 0.5 g/40 mL respectively. The centrifuge tubes were placed on a rotary shaker at 80 rpm for 24 h and then centrifuged using a Sartorius Sigma 4-16 at 9500 rpm for 20 min before the supernatants were passed through a Whatman No. 42 filter paper. The residual MB and DR 80 in the solutions after adsorption were measured using a Cary 50 Probe UV Visible Spectrophotometer at 665 nm and 543 nm wavelengths, respectively. All experiments were conducted in triplicate.

The Langmuir and Freundlich sorption isotherm

models were used to fit the sorption data. The linearized Langmuir's adsorption model used was as follows:

$$\frac{C_e}{q_e} = \frac{1}{q_m K_L} + \frac{C_e}{q_m} \quad (3)$$

Where C<sub>e</sub> is the concentration of adsorbate at equilibrium (mg/L), q<sub>e</sub> is the adsorption capacity at equilibrium (mg/g), K<sub>L</sub> is the Langmuir constant related to adsorption capacity (mg/g) and q<sub>m</sub> is the adsorption capacity (mg/g). The essential characteristics of the Langmuir isotherm can be expressed by a dimensionless constant called the separation factor (R<sub>L</sub>). R<sub>L</sub> was calculated as:

$$R_L = \frac{1}{1 + K_L C_0} \quad (4)$$

where K<sub>L</sub> is the Langmuir constant and C<sub>0</sub> is the highest initial dye concentration (mg/L). The value of R<sub>L</sub> indicates whether the type of isotherm is favourable (0 < R<sub>L</sub> < 1), linear (R<sub>L</sub> = 1), unfavourable (R<sub>L</sub> > 1), or irreversible (R<sub>L</sub> = 0) [30]. The linear form of the Freundlich isotherm is as follows:

$$\log q_e = \log K_F + \frac{1}{n} \log C_e, \quad (5)$$

where K<sub>F</sub> is the adsorption capacity (L/mg), 1/n is the adsorption intensity, q<sub>e</sub> is the adsorption capacity at equilibrium (mg/g), and C<sub>e</sub> is the concentration of adsorbate at equilibrium (mg/L).

## RESULTS AND DISCUSSION

### 1. Characterisation of Adsorbents

#### 1.1. Physical Properties

The ash content values for the adsorbents are presented in Table 1. The ash contents were low and the values varied among the adsorbents studied. The ash content values increased in the order: A-EFBB (5.05%) < Fe-EFBB (5.83%) < B-EFBB (7.14%) < EFBB (14.73%) < AC (17.16%). The results indicate that chemical modification reduced the ash content of EFBB by more than half. Meanwhile, the ash content of AC was the highest among the adsorbents. The EFBB used in this study was produced via a slow pyrolysis process. This explains its expected lower ash content, as lower temperatures produce lower ash content values in biochar [31]. The modified EFBBs had lower ash values because alkali, acid and oxidizing agent treatments removed the inorganic fractions from the original EFBB. Even though the activated carbon used in this study was produced from acid-washed lignite carbon, it was pyrolyzed under high temperatures. Hence, the resulting ash content is higher compared to the other adsorbents.

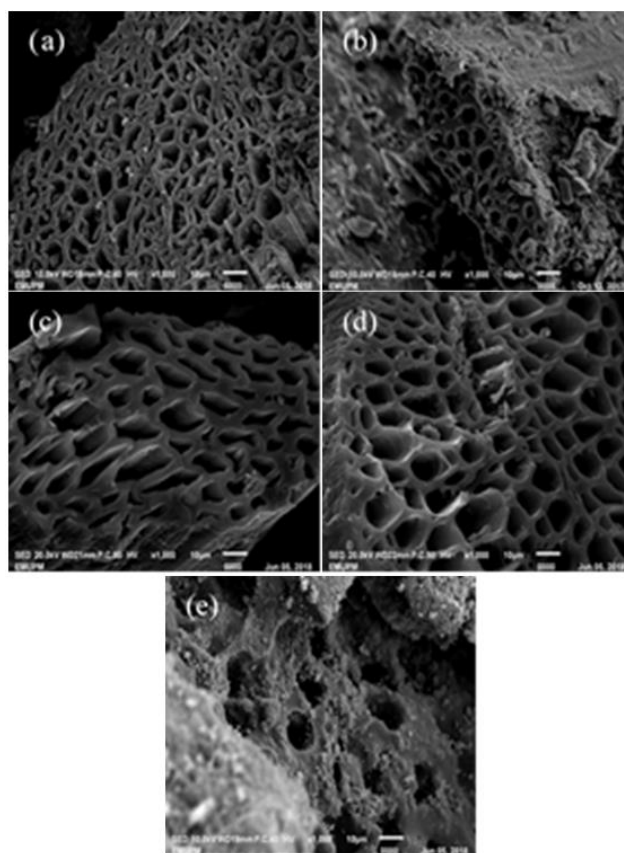
**Table 1.** Physical Properties of Adsorbent.

Physical Properties	AC	EFBB	FE-EFBB	A-EFBB	B-EFBB
Ash Content (%)	17.16	14.73	5.83	5.05	7.14
BET Surface Area ( $\text{m}^2/\text{g}$ )	522.32	0.79	2.92	0.89	1.06
Pore Volume ( $\text{m}^3/\text{g}$ )	0.60	0.30	0.13	0.31	0.37

The BET surface areas and pore volumes of all the adsorbents are listed in Table 1. Based on the results, chemical modification increased the surface area of EFBB. The BET surface area increased in the following order: EFBB ( $0.7883 \text{ m}^2/\text{g}$ ) < A-EFBB ( $0.8895 \text{ m}^2/\text{g}$ ) < B-EFBB ( $1.0637 \text{ m}^2/\text{g}$ ) < Fe-EFBB ( $2.9208 \text{ m}^2/\text{g}$ ) < AC ( $522.3249 \text{ m}^2/\text{g}$ ). It was apparent that the surface area of AC was much higher compared to the rest of the adsorbents. On the other hand, the pore volumes followed the order: FE-EFBB ( $0.13 \text{ m}^3/\text{g}$ ) < EFBB ( $0.30 \text{ m}^3/\text{g}$ ) < A-EFBB ( $0.31 \text{ m}^3/\text{g}$ ) < B-EFBB ( $0.37 \text{ m}^3/\text{g}$ ) < AC ( $0.60 \text{ m}^3/\text{g}$ ). Acid and alkaline treatments slightly increased the pore volume of EFBB, but treating EFBB with  $\text{FeCl}_3$  reduced its pore volume. Exposing biochar to acidic solutions such as  $\text{H}_2\text{SO}_4$  develops carboxylic groups as well as micropores on the biochar's surface, which lead to an increase in surface area [35-37]. However, the pore volume of EFBB was reduced when activated with  $\text{FeCl}_3$  perhaps because the EFBB pores were clogged by iron particles, as reported by Sizmur et al. (2017) [38]. AC had the highest pore volume compared to the other EFBBs and similar results were reported by Ayawei et al. (2017) who found that the AC from unwashed lignite carbon used in their study had the highest surface area compared to biochars produced from Korean cabbage, rice straw and wood chips [32].

Sewu et al. (2017) reported a BET surface area of  $1.478 \text{ m}^2/\text{g}$  and a total pore volume of  $0.035 \text{ cm}^3/\text{g}$  for raw oil palm empty fruit bunches [33]. The values are comparable with the data obtained in the current study which show that EFBBs have low surface areas and pore volumes as the biochar feedstock has the same characteristics. Rebitan et al. (2012) who studied the chemical modification of biochar reported that chemical modification using acids, alkalis and oxidizing agents increased the surface area of the biochar [34]. Liu et al. (2102) produced acid- and alkali-modified biochar by chemically activating rice husk biochar using  $\text{H}_2\text{SO}_4$  and  $\text{KOH}$  [6]. The surface area and micropore volume of the acid activated biochar were  $46.8 \text{ m}^2/\text{g}$  and  $0.033 \text{ cm}^3/\text{g}$ , while the values for the alkali activated biochar were  $117.8 \text{ m}^2/\text{g}$  and  $0.073 \text{ cm}^3/\text{g}$ , respectively. These values were higher than the surface area and micropore volume recorded for the raw biochar, which were  $34.4 \text{ m}^2/\text{g}$  and  $0.028 \text{ m}^3/\text{g}$ , respectively. As with the above results, activation of EFBB with  $\text{FeCl}_3$ ,  $\text{H}_2\text{SO}_4$  and  $\text{KOH}$  in the present study was found to increase its surface area and pore volume (Table 1).

SEM images of all the adsorbents are shown in Figure 1. The surface structure of AC was rough, with large, irregular pores. This was evidently reflected by its high BET surface area and pore volume. However, EFBB and its chemically-modified variants exhibited a distinguishable honeycomb-like framework due to the presence of tubular structures originally emanating from plant cells. As a consequence of these well-developed pores, all EFBBs possessed high BET surface areas [18]. In general, all the modified EFBBs showed no, or very little, evidence of clogged pores on their surfaces which may be due to the removal of the ash during the modification process (Table 1). Further, modification of EFBB by acid and alkali treatment caused its surface to become smoother and develop larger, irregular-sized pores.

**Figure 1.** SEM Images of (a) EFBB, (b) Fe-EFBB, (c) A-EFBB, (d) B-EFBB, (e) AC.

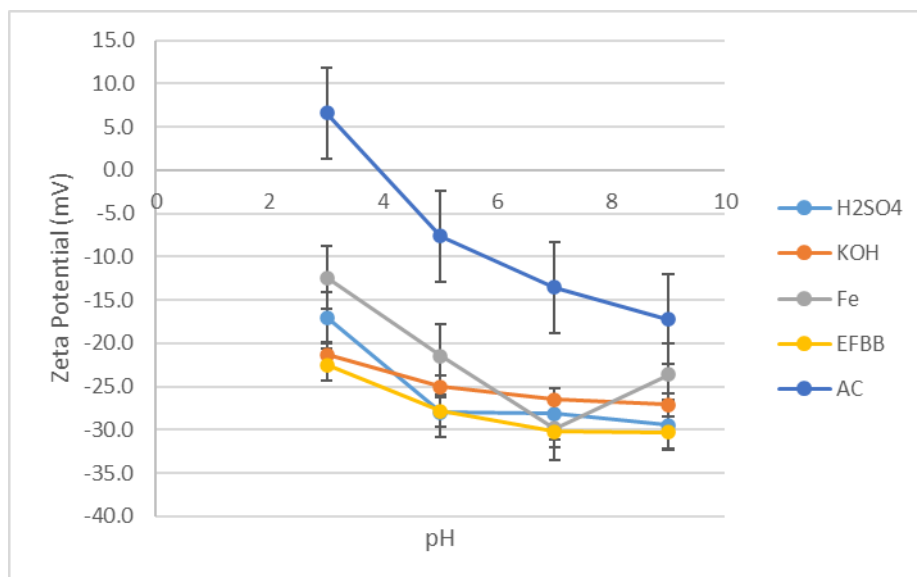


**Figure 2.** Zeta Potential of Adsorbents.

**Table 2.** Chemical Properties of Adsorbents.

Chemical properties	AC	EFBB	Fe-EFBB	A-EFBB	B-EFBB
pH	6.07	7.73	6.55	4.61	7.01
EC ( $\mu\text{S}/\text{cm}$ )	100.0	746.33	103.8	59.1	302.7
Exchangeable bases ( $\text{cmol}_\text{c}/\text{kg}$ )					
Ca <sup>2+</sup>	0.66	7.90	0.47	0.2249	0.7160
Mg <sup>2+</sup>	0.57	7.42	1.16	0.0194	0.29275
K <sup>+</sup>	5.02	12.39	3.18	2.2898	6.9217
Elemental composition (%)					
C	69.48	62.26	66.37	60.56	68.95
H	0.29	3.50	3.54	3.41	3.364
N	0.03	0.54	0.98	0.6078	0.6227
S	0.38	0.77	0.54	0.3609	0.6201
O	29.82	32.93	28.58	35.06	26.44
H/C molar ratio	0.004	0.056	0.053	0.056	0.049
O/C molar ratio	0.429	0.529	0.431	0.579	0.383
(O+N)/C	0.430	0.538	0.445	0.589	0.392
Acid functional groups ( $\text{meq}/\text{g}$ )					
Total acidic groups	0.94	0.70	1.94	2.55	0.99
Carboxylic groups	0.52	0.25	0.64	0.95	0.64
Lactonic groups	0	0	0	0	0
Phenolic groups	0.42	0.45	1.30	1.60	0.35
Iodine number ( $\text{mg}/\text{g}$ )	780.73	61.23	90.25	88.38	101.28

## 1.2. Chemical Properties

The zeta potential of all adsorbents at different pH values are shown in Figure 2. The zeta potentials of all adsorbents were negative over the whole pH range except for AC at pH 3, indicating that negative charges were dominant on the surfaces of the adsorbents [39, 40]. The zeta potentials of the chemically modified biochars were less negative compared to the unmodified EFBBs while AC had the highest zeta potential among all the adsorbents over the pH range of 3 to 9 (Figure 2). This implies that the surface of AC was less negatively-charged than all the EFBBs. The zeta potentials of the chemically-modified EFBBs were less negative than that of EFBB, suggesting that deprotonation of the carboxylic and hydroxyl functional groups decreased after chemical modification, and the functional groups could have interacted with the  $H^+$ ,  $K^+$  or  $Fe^{3+}$  that were present in the solution. Among the adsorbents studied, AC had the least negative surface charge over this pH range because all the EFBBs used in this study were pyrolyzed at lower temperatures while AC was produced at high temperatures, hence the EFBBs contained more functional groups which could be deprotonated [42].

The elemental composition of all the adsorbents are shown in Table 2. Generally, a clear pattern was observed where all the adsorbents contained C and O as their two major elements. The high C content of the EFBBs make them suitable as adsorbents for the removal of dyes [42].

However, the total C content of the EFBBs were slightly lower compared to AC indicating that the EFBBs were less carbonized [43]. Acid modification via  $H_2SO_4$  increased the oxygen content, which resulted in high surface aromaticity (higher H/C), high stability (higher O/C) and lower hydrophobicity [44]. Furthermore, the A-EFBB had the lowest C content, highest O content, and the highest H/C and O/C ratios, which make it a good adsorbent for aqueous contaminants [45]. Meanwhile, KOH and  $FeCl_3$  treatment increased the carbon content of EFBB while reducing the O content, resulting in low H/C and O/C values for B-EFBB and Fe-EFBB. Alkali and  $FeCl_3$  activation reduced the aromaticity but increased the aromaticity of the resulting biochars [46].

The pH values of the adsorbents are listed in Table 2. The unmodified EFBB had the highest pH while A-EFBB had the lowest, but the pH values of both Fe-EFBB and B-EFBB were not significantly

different from that of EFBB. The pH of AC was lower than that of EFBB, Fe-EFBB and B-EFBB, but higher than that of A-EFBB. The commercial AC used in this study displayed a weakly acidic pH value (6.07) which was higher than the value of 5.5 reported by Ma et al. (2014) for a commercial activated carbon in their study [47]. In the production process, AC was acid washed which could be the reason for the slightly lower pH values recorded in this study compared to the rest of adsorbents except for A-EFBB. Empty fruit bunch biomass generally has a neutral to slightly alkaline character with pH values ranging from 7.20 to 7.80 [48, 42]. Therefore, biochar produced from the same biomass would display similar or higher pH values. After chemical modification, the biochars were washed with deionized water until the pH of the elution water was 7.0, and this is probably why the Fe-EFBB and B-EFBB pH values were lower than that of the unmodified EFBB. A pH value of 4.61 was recorded for A-EFBB due to the acidity of the sulphuric acid solution. Biochar modification using  $H_2SO_4$  leads to more acidic functional groups on its surface, thus A-EFBB had more carboxylic groups containing oxygen [49, 50].

The FTIR spectra of all the adsorbent samples are shown in Figure 3 while the band positions and their related functional groups are listed in Table 3. The AC spectrum had a peak at  $765.27\text{ cm}^{-1}$  attributed to aromatic  $-CH$  stretching while the peaks at  $1114.28$  and  $1458.81\text{ cm}^{-1}$  were due to the  $-COOH$  bending vibration,  $C=O$  stretching of aryl-alkyl and  $C=C$  vibration. The  $-CH$  stretching vibration of asymmetric aliphatic  $-CH$ ,  $-CH_2$  and  $-CH_3$  in the AC were represented by the peak at  $2910.18\text{ cm}^{-1}$  while the band at  $3353.65\text{ cm}^{-1}$  is typical of the  $-OH$  stretching/isolated or exchangeable functional group. The spectrum for EFBB displayed characteristics of the common polymeric plant-based materials cellulose, hemicellulose and lignin, at  $763.01 - 768.89\text{ cm}^{-1}$ ,  $1108.63 - 1166.32\text{ cm}^{-1}$  and  $1357.55 - 1379.07\text{ cm}^{-1}$  respectively. The band around  $3100 - 3500\text{ cm}^{-1}$  found in the EFBB spectrum signifies the presence of a hydroxyl (O-H) stretching vibration. After chemical modification, the hydroxyl (O-H) stretching vibration peaks shifted to  $3373.25\text{ cm}^{-1}$ ,  $3175.83\text{ cm}^{-1}$  and  $3367.59\text{ cm}^{-1}$  for Fe-EFBB, B-EFBB and A-EFBB respectively, suggesting that chemical modification had taken place on the surface of EFBB. The O-H stretching peaks detected for chemically-modified EFBBs were broader, while the peaks were sharper and more intense on the AC, indicating that AC had free O-H groups while chemically-modified EFBBs had H bonded O-H groups [6, 32, 51].

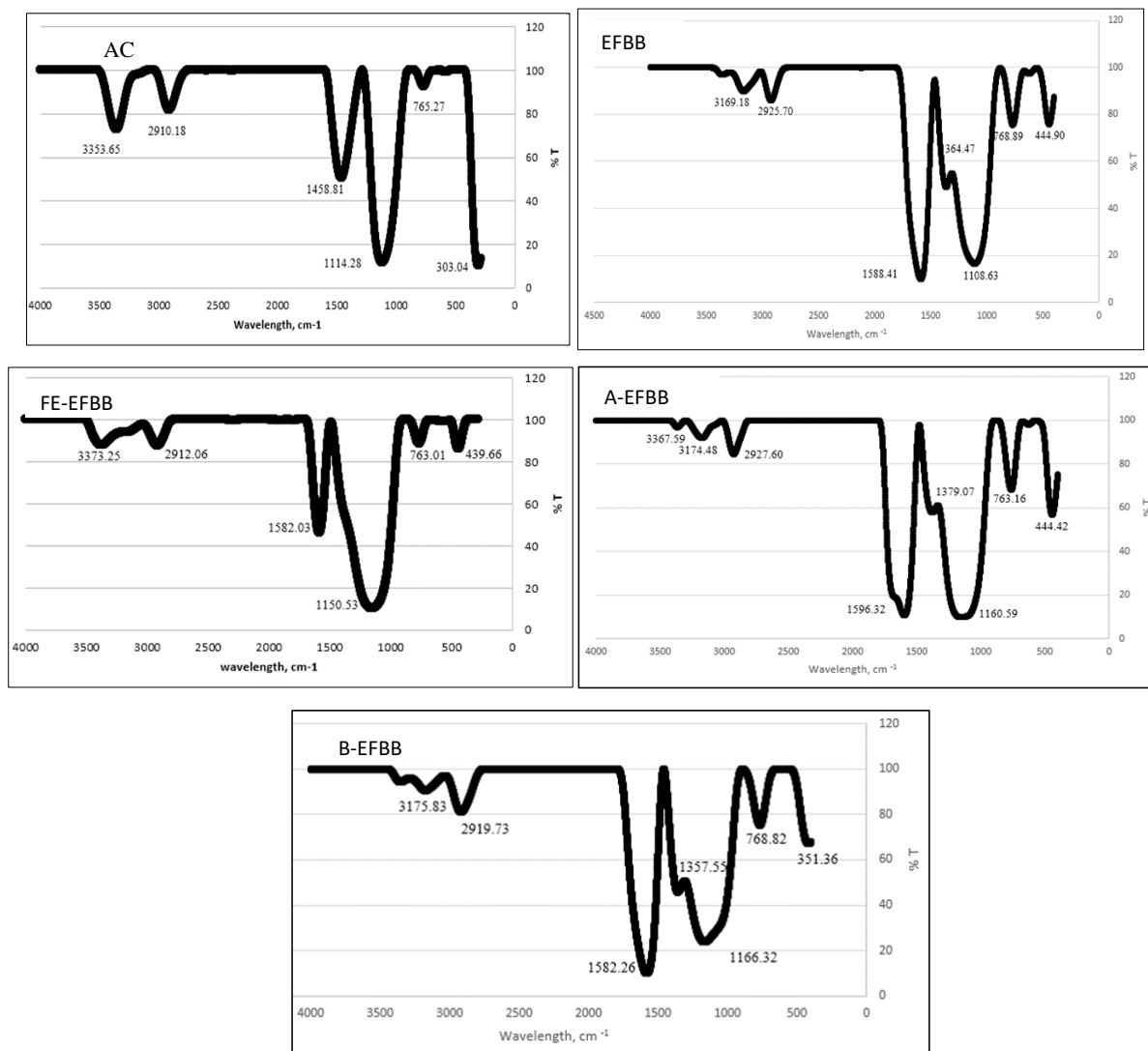


Figure 3. FTIR Plots of Adsorbents.

The unmodified EFBB showed a peak at 2925.70, which suggests the presence of a  $\text{CH}_3$  group stretching vibration. The peaks were shifted to 2912.06  $\text{cm}^{-1}$ , 2919.73  $\text{cm}^{-1}$ , and 2927.60  $\text{cm}^{-1}$  in the spectra of Fe-EFBB, B-EFBB and A-EFBB, respectively. The  $\text{CH}_3$  stretching vibration peak for AC at 2910.18  $\text{cm}^{-1}$  was observed to be slightly stronger and sharper when compared with the other adsorbents. The peak at 1588.41  $\text{cm}^{-1}$  in the EFBB spectrum indicates the presence of asymmetric  $\text{COO}^-$  stretching of the carboxylic salt. After chemical modification, the peak shifted to 1582.03  $\text{cm}^{-1}$ , 1582.26  $\text{cm}^{-1}$ , and 1596.32  $\text{cm}^{-1}$  in the Fe-EFBB, A-EFBB and B-EFBB spectra, respectively. As for AC, the peak detected at 1458.81  $\text{cm}^{-1}$  could be attributed to  $\text{C}=\text{C}$  aromatic ring stretching [38, 42]. Table 3 lists all the surface functional groups present in all the adsorbents. It is evident that functional groups on the chemically-activated EFBB

varied depending on the chemicals used.

Total acidity values followed the ascending order: EFBB (0.70 meq/g) < AC (0.94 meq/g) < B-EFBB (0.99 meq/g) < Fe-EFBB (1.94 meq/g) < A-EFBB (2.25 meq/g), and they were dominated by carboxylic and phenolic groups. Based on the total acidity values and the FTIR spectra, the EFBB total acidity as well as the carboxyl groups increased after chemical modification. Meanwhile, no lactone functional groups were detected in any of the adsorbents. Chemical modification significantly increased the number of carboxylic groups in the EFBBs. After chemical modification, phenolic groups significantly increased in A-EFBB and Fe-EFBB. There were significant increases in the total acidity values for A-EFBB and Fe-EFBB but no significant increase was recorded for B-EFBB after chemical modification.

**Table 3.** Functional Groups of Adsorbents.

Functional groups	Band Positions (cm <sup>-1</sup> )				
	AC	EFBB	FE-EFBB	A-EFBB	B-EFBB
O-H stretching	3353.65	3169.18	3373.25	3367.59 3174.48	3175.83
Aliphatic C-H stretching	2910.18	2952.70	2912.06	2927.60	2919.73
–COOH bending vibration, C=O stretching of aryl-alkyl, C=C and S=O bonds	1114.28 1458.81	1588.41	1582.03	1582.26	1596.32
Aromatic C-H stretching	765.27				
cellulose		763.01–768.89			
hemicellulose		1108.63–1166.32			
lignin		1357.55–1379.07			

## 2. Adsorption Isotherm

Figure 4 (a) and (b) show the equilibrium adsorption isotherm plots of both MB and DR 80 dyes by the various adsorbents. All the plots form L-curves, which suggests a monolayer adsorption on the homogenous surface of the adsorbents [52]. In general, adsorption increased as the concentration of both dyes increased. The linearized Langmuir and Freundlich adsorption isotherm plots for both MB and DR 80 dyes onto different adsorbents are shown in Figure 5 (a)-(d) and the isotherm constants and correlation coefficients of the plots are presented in Table 4. Although the adsorption data fit both the Langmuir and Freundlich isotherm models well, the Langmuir model exhibited a slightly better data fit than the Freundlich model based on their  $R^2$  values (Table 4). The results of this study are in accordance with those of Ayawei et al. (2017) [32]. They reported that the adsorption of an anionic dye (Congo red) and a cationic dye (crystal violet) by biochars produced from Korean cabbage, rice straw and woodchips, fit the Langmuir isotherm better than the Freundlich isotherm, suggesting that adsorption of the dyes onto the biochars were homogenous and occurred on the surface of the adsorbents. Wong et al. (2004) [53] also reported that adsorption of MB by switchgrass biochar pyrolyzed at two different temperatures (600 and 900°C) were better described by the Langmuir than the Freundlich adsorption model. The Langmuir model's maximum adsorptive capacity values ( $q_m$ ) for MB by the adsorbents followed the increasing order: EFBB (6.14 mg/g) < FE-EFBB (10.13 mg/g) < B-EFBB (76.34 mg/g) < A-EFBB (125 mg/g) < AC (136.99 mg/g). For DR 80, the maximum adsorptive capacity values ( $q_m$ ) followed the increasing order: EFBB (1.15 mg/g) < FE-EFBB (4.71 mg/g) < A-EFBB (40.16 mg/g) < B-EFBB (78.13 mg/g) < AC (116.28 mg/g), as shown in Table 4. Based on these results, the chemically modified EFBBs

showed higher adsorption capacities for both MB and DR 80 compared to the unmodified EFBB. However, AC was the best adsorbent for both dyes, with adsorption capacities of 136.99 mg/g and 116.28 mg/g for MB and DR 80, respectively. The  $R_L$  values for all the adsorbents were between 0 and 1 indicating that the adsorption processes were favourable [30]. Meanwhile, the Freundlich adsorption capacity ( $K_F$ ) followed the ascending order: EFBB < Fe-EFBB < B-EFBB < A-EFBB < AC for MB, while for DR 80, the order was: EFBB < Fe-EFBB < A-EFBB < B-EFBB < AC.

The Langmuir plots for both dyes in Figure 5 (a) and (c) showed that AC was the best adsorbent, likely because it had the largest surface area and pore volume (Table 1) as well as a highly porous structure, as can be observed in the SEM micrograph (Figure 1). These attributes suggest more sites are available for the dyes to be adsorbed. Ayawei et al. (2017) reported that AC was the best adsorbent for Congo Red dye removal when compared to other adsorbents, including different types of biochars [32]. He attributed this finding to the large surface area and mesoporous nature of AC. The adsorption isotherm plots (Figure 4) also showed that unmodified EFBB had the least adsorption capacity for both dyes compared to the other adsorbents. This could be due to several reasons. The ash content of EFBB was higher than those of the chemically-modified EFBBs. The higher ash content may have blocked or filled the micropores on the unmodified EFBB and hindered the adsorption process of both dyes. According to Park et al. (2019) [54], during the dye adsorption process, dye molecules must first encounter the external boundary layer, then diffuse from the boundary layer film onto the adsorbent surface, and finally into the porous structure of the adsorbents. EFBB also recorded the lowest surface area value (Table 1), which could also be a reason for its lowest adsorption capacity value ( $q_m$ ).



Moreover, Saad et al. (2007) stated that higher ash content indicates higher inorganics and higher pH [55]. Therefore, there is a higher possibility of ionic exchange

and chemical interactions instead of physical interactions. This could be a reason for the higher  $q_m$  value of EFBB for MB compared to DR 80 (Table 4).

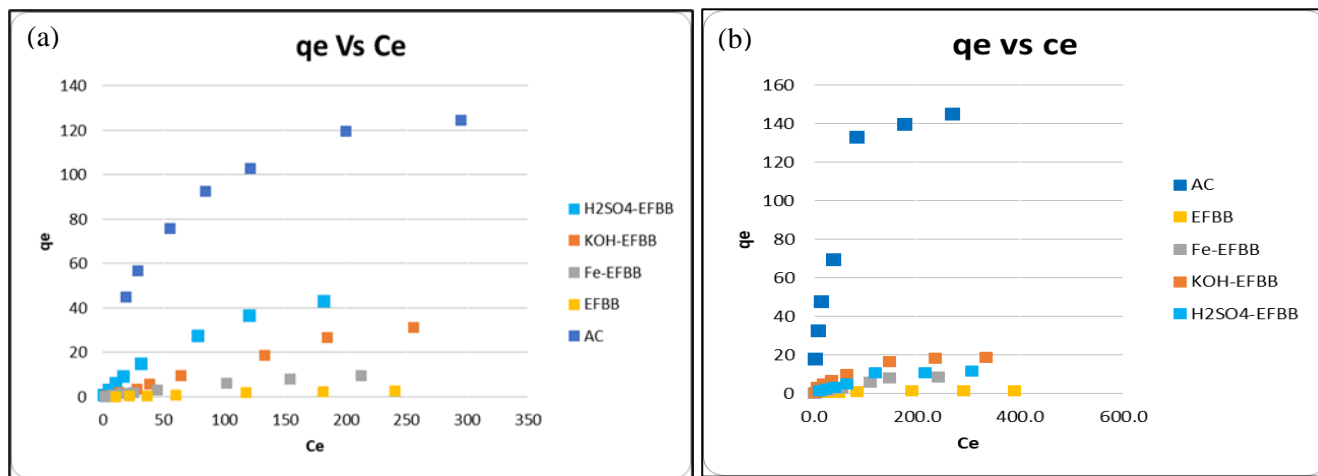


**Figure 4.** Adsorption Isotherm Plots for (a) Methylene blue and (b) Direct Red 80.

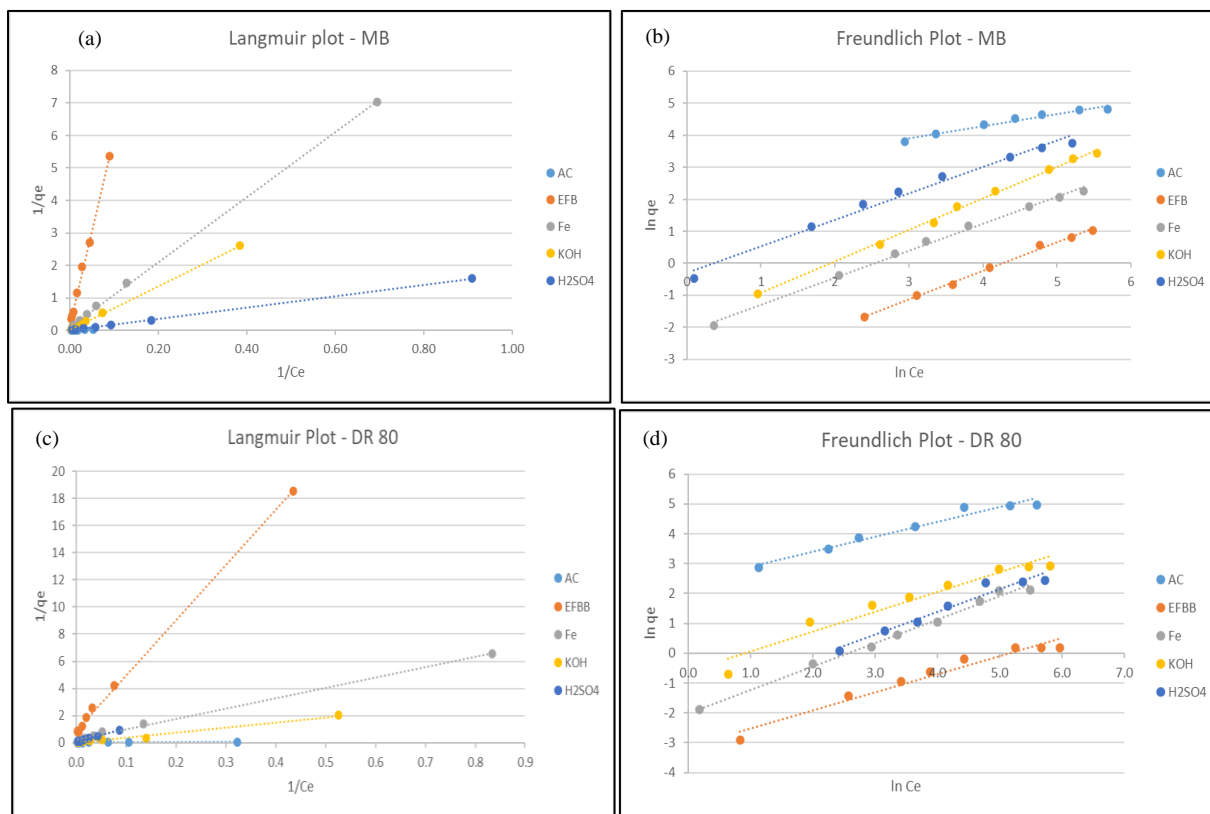


**Figure 5.** Langmuir and Freundlich Linear Plots of Methylene Blue and Direct Red 80 Respectively. Plots (a) and (b) represent Langmuir and Freundlich Plots of MB, while (c) and (d) represent Langmuir and Freundlich Plots of DR 80.

**Table 4.** Adsorption Isotherm Model.

Dyes	Adsorbent s	Langmuir		$R^2$	$R_L$	Freundlich		
		$K_L$ (L/mg)	$Q_m$ (mg/g)			$K_F$ (mg/g)	$n$	$R^2$
Methylene Blue	AC	0.0249	136.99	0.9955	0.0819	15.79	0.3806	0.9704
	EFBB	0.1066	6.14	0.9970	0.0204	0.02	0.8915	0.9962
	Fe-EFBB	0.0098	10.13	0.9997	0.5156	0.12	0.8424	0.9958
	A-EFBB	0.0046	125.00	0.9998	0.3257	1.04	0.7404	0.9898
	B-EFBB	0.0019	76.34	0.9994	0.8260	0.15	0.9848	0.9971
Direct Red 80	AC	0.0546	116.28	0.9679	0.0391	11.11	0.4965	0.9631
	EFBB	0.0213	1.15	0.9986	0.0944	0.04	0.6116	0.9591
	Fe-EFBB	0.0276	4.71	0.9966	0.0745	0.13	0.7827	0.9932
	A-EFBB	0.0050	40.16	0.9926	0.3076	0.38	0.7609	0.9557
	B-EFBB	0.0034	78.13	0.9868	0.3953	0.54	0.6662	0.9411

The Langmuir's maximum  $q_m$  for A-EFBB was higher than that for unmodified EFBB and the other chemically-modified EFBBs. Although A-EFBB had a lower surface area and porosity compared to B-EFBB (Table 1), the  $q_m$  value of A-EFBB was higher than that of B-EFBB. This may be attributed to the higher O content (35.06%) and carboxylic groups (0.95 meq/g) in A-EFBB, which indicates that the surface acidic groups may play a major role in the adsorption mechanism, as suggested by Valix et al. (2004) [56]. Oxygen containing functional groups are usually negatively-charged in solution, which may result in attractive electrostatic interactions between the cationic MB dye and the surface of A-EFBB. However, adsorption of A-EFBB to the anionic DR 80 was poor likely because of the repulsive electrostatic interaction [57, 58]. Hence A-EFBB, which contained the highest number of carboxylic groups among the adsorbents (Table 2), showed a stronger adsorption to the cationic dye but poorly adsorbed the anionic dye.

Chemical modification of biochar with alkali produces a positively-charged biochar which in turn assists in adsorbing negatively charged species [34]. Thus, KOH modification enabled the formation of a hydroxyl (-OH) functional group on the surface of B-EFBB, which is responsible for its slightly basic pH (Table 2). Therefore, the adsorption of the anionic DR 80 by B-EFBB was higher than the adsorption by A-EFBB and the unmodified EFBB (Table 4). Gong et al. (2005) studied the adsorption of anionic dyes (Reactive Black 5 and Congo Red) onto coffee waste modified with polyethylenimine (PEI) and found that the highest adsorption recorded was due to the formation of attractive electrostatic interactions between positively-charged amine groups on the PEI-CW surface and negatively charged anionic dyes [59].

The zeta potential values of Fe-EFBB were all

less than zero throughout the studied pH range, indicating that Fe-EFBB was negatively charged. The negatively charged Fe-EFBB would have developed an electrostatic attraction to the cationic MB, hence improving the adsorption capacity of Fe-EFBB compared to the unmodified EFBB. However, the negatively charged Fe-EFBB would have been electrostatically repulsed by the anionic DR 80 and therefore the  $q_m$  value of Fe-EFBB was lower than that of the unmodified EFBB (Table 4). Wong et al. (2020) also found similar results on the effects of coating an acid-treated biochar with magnetic  $Fe_3O_4$  nanoparticles [60].

## CONCLUSIONS

In this study, the chemically-modified biochars A-EFBB, B-EFBB, and Fe-EFBB showed enhanced adsorption capacities towards commercial dyes (MB and DR 80) compared to unmodified EFBB. This could be attributed to a lower ash content, increased BET surface areas and pore volumes, surface aromaticity and the presence of functional groups. However, AC showed the highest adsorption capacity compared to the rest of adsorbents due to its largest surface area and pore volume. A-EFBB showed a higher affinity towards MB than B-EFBB and Fe-EFBB due to the high O content and carboxylic groups in A-EFBB. On the other hand, B-EFBB showed a higher affinity towards DR 80, as chemical modification with KOH enabled the formation of a hydroxyl (-OH) functional group on its surface. Hence, these findings prove that chemically-modified biochars have good potential to be cheap and effective adsorbents that are almost equivalent to the highly efficient but expensive commercial AC. The experimental results for the removal of both MB and DR 80 dyes in this study were limited to a maximum concentration of 450 mg/L to fit lab scale experiments and only one type of low-cost adsorbent was used.

However, the concentrations of dye contaminants in the environment are generally much higher and their impact much greater. Therefore, the utilisation of low-cost adsorbents should be explored further, with higher concentrations of dye pollutants, to test the efficiency of this method on a larger scale.

#### CONFLICT OF INTEREST

All the authors do not have any conflicts of interest.

#### ACKNOWLEDGEMENT

The authors would like to thank Universiti Putra Malaysia for providing the funds to carry out this study under the UPM/IPS/9527200 Research Grant.

#### REFERENCES

1. Afroz, R. & Rahman, A. (2017) Health impact of river water pollution in Malaysia. **4(5)**, 78–85.
2. Sundarajoo, A. & Maniyam, M. N. (2020) Enhanced Decolourization of Congo Red Dye by Malaysian Rhodococcus UCC 0010 Immobilized in Calcium Alginate Enhanced Decolourization of Congo Red Dye by Malaysian Rhodococcus UCC 0010 Immobilized in Calcium Alginate. 1 (February), 1–9.
3. Idris, A., Hashim, R., Rahman, R. A., Ahmad, W. A., Ibrahim, Z., Razak, P. R. A., Zin, H. M., & Bakar, I. (2007) Application of Bioremediation Process for Textile Wastewater Treatment Using Pilot Plant. *International Journal of Engineering and Technology*, **4(2)**, 228–234.
4. Pang, Y. L. & Abdullah, A. Z. (2013) Current status of textile industry wastewater management and research progress in Malaysia: A review. *Clean - Soil, Air, Water*, **41(8)**, 751–764. <https://doi.org/10.1002/clen.201000318>
5. Sajab, M. S., Chia, C. H., Zakaria, S., Jani, S. M., Ayob, M. K., Chee, K. L., Khiew, P. S. & Chiu, W. S. (2011) Citric acid modified kenaf core fibres for removal of methylene blue from aqueous solution. *Bioresource Technology*, **102(15)**, 7237–7243. <https://doi.org/10.1016/j.biortech.2011.05.011>
6. Liu, P., Liu, W. J., Jiang, H., Chen, J. J., Li, W. W. & Yu, H. Q. (2012) Modification of bio-char derived from fast pyrolysis of biomass and its application in removal of tetracycline from aqueous solution. *Bioresource Technology*, **121**, 235–240. <https://doi.org/10.1016/j.biortech.2012.06.085>
7. Zheng, Y., Chen, D., Li, N., Xu, Q., Li, H., He, J. & Lu, J. (2017) Highly efficient simultaneous adsorption and biodegradation of a highly-concentrated anionic dye by a high-surface-area carbon-based biocomposite. *Chemosphere*, **179**, 139–147. <https://doi.org/10.1016/j.chemosphere.2017.03.096>
8. Corso, C. R. & Maganha De Almeida, A. C. (2009) Bioremediation of dyes in textile effluents by *aspergillus oryzae*. *Microbial Ecology*, **57(2)**, 384–390. <https://doi.org/10.1007/s00248-008-9459-7>
9. Salleh, M. A. M., Mahmoud, D. K., Karim, W. A. W. A. & Idris, A. (2011) Cationic and anionic dye adsorption by agricultural solid wastes: A comprehensive review. *Desalination*, **280(1–3)**, 1–13. <https://doi.org/10.1016/j.desal.2011.07.019>
10. Thines, K. R., Abdullah, E. C., Mubarak, N. M. & Ruthiraan, M. (2017) Synthesis of magnetic biochar from agricultural waste biomass to enhancing route for waste water and polymer application: A review. *In Renewable and Sustainable Energy Reviews*. <https://doi.org/10.1016/j.rser.2016.09.057>
11. Senthilkumaar, S., Varadarajan, P. R., Porkodi, K., & Subbhuraam, C. V. (2005) Adsorption of methylene blue onto jute fiber carbon: Kinetics and equilibrium studies. *Journal of Colloid and Interface Science*, **284(1)**, 78–82. <https://doi.org/10.1016/j.jcis.2004.09.027>
12. De Jesus da Silveira Neta, J., Costa Moreira, G., da Silva, C. J., Reis, C. & Reis, E. L. (2011) Use of polyurethane foams for the removal of the Direct Red 80 and Reactive Blue 21 dyes in aqueous medium. *Desalination*, **281(1)**, 55–60. <https://doi.org/10.1016/j.desal.2011.07.041>
13. Saleem, M., Pirzada, T. & Qadeer, R. (2007) Sorption of acid violet 17 and direct red 80 dyes on cotton fiber from aqueous solutions. *Colloids and Surfaces A: Physicochemical and Engineering Aspects*, **292(2–3)**, 246–250. <https://doi.org/10.1016/j.colsurfa.2006.06.035>
14. Doulati Ardejani, F., Badii, K., Limaee, N. Y., Shafaei, S. Z. & Mirhabibi, A. R. (2008) Adsorption of Direct Red 80 dye from aqueous solution onto almond shells: Effect of pH, initial concentration and shell type. *Journal of Hazardous Materials*, **151(2–3)**, 730–737. <https://doi.org/10.1016/j.jhazmat.2007.06.048>
15. Pathania, D., Sharma, S. & Singh, P. (2013) Removal of methylene blue by adsorption onto activated carbon developed from *Ficus carica* bast. *Arabian Journal of Chemistry*, **10**, S1445–S1451. <https://doi.org/10.1016/j.arabjc.2013.04.021>

16. Bharathi, K. S. & Ramesh, S. T. (2013) Removal of dyes using agricultural waste as low-cost adsorbents: a review. *Applied Water Science*, **3**(4), 773–790. <https://doi.org/10.1007/s13201-013-0117-y>
17. Boehm, H. (1994) Some aspects of the surface chemistry of carbon blacks and other carbons. *Pergamon*, **32**(5), 759–769.
18. Chen, B., Chen, Z. & Lv, S. (2011) A novel magnetic biochar efficiently sorbs organic pollutants and phosphate. *Bioresource Technology*, **102**(2), 716–723. <https://doi.org/10.1016/j.biortech.2010.08.067>
19. Nartey, O. D. & Zhao, B. (2014) Biochar preparation, characterization, and adsorptive capacity and its effect on bioavailability of contaminants: An overview. *Advances in Materials Science and Engineering*, **12**. <https://doi.org/10.1155/2014/715398>
20. Rajapaksha, A. U., Chen, S. S., Tsang, D. C. W., Zhang, M., Vithanage, M., Mandal, S., Gao, B., Bolan, N. S. & Ok, Y. S. (2016) Engineered/designer biochar for contaminant removal/immobilization from soil and water: Potential and implication of biochar modification. *Chemosphere*, **148**, 276–291. <https://doi.org/10.1016/j.chemosphere.2016.01.043>
21. Tan, G., Sun, W., Xu, Y., Wang, H. & Xu, N. (2016) Sorption of mercury (II) and atrazine by biochar, modified biochars and biochar based activated carbon in aqueous solution. *Bioresource Technology*, **211**, 727–735. <https://doi.org/10.1016/j.biortech.2016.03.147>
22. Sajab, M. S., Chia, C. H., Zakaria, S. & Khiew, P. S. (2013) Cationic and anionic modifications of oil palm empty fruit bunch fibers for the removal of dyes from aqueous solutions. *Bioresource Technology*, **128**, 571–577. <https://doi.org/10.1016/j.biortech.2012.11.010>
23. Huang, H., Tang, J., Gao, K., He, R., Zhao, H. & Werner, D. (2017) Characterization of KOH modified biochars from different pyrolysis temperatures and enhanced adsorption of antibiotics. *RSC Advances*, **7**(24), 14640–14648. <https://doi.org/10.1039/c6ra27881g>
24. Samsuri, Abd Wahid, Sadegh-zadeh, F. & Sehbardan, B. J. (2013) Adsorption of As ( III ) and As ( V ) by Fe coated biochars and biochars produced from empty fruit bunch and rice husk. *Biochemical Pharmacology*, **1**(4), 981–988. <https://doi.org/10.1016/j.jece.2013.08.009>
25. Savova, D., Apak, E., Ekinci, E., Yardim, F., Petrov, N., Budinova, T., Razvigorova, M. & Minkova, V. (2001) Biomass conversion to carbon adsorbents and gas. *Biomass and Bioenergy*, **21**(2), 133–142. [https://doi.org/10.1016/S0961-9534\(01\)00027-7](https://doi.org/10.1016/S0961-9534(01)00027-7)
26. Claoston, N., Samsuri, A., And, M. A. H. & Amran, M. M. (2014) Effects of pyrolysis temperature on the physicochemical properties of empty fruit bunch and rice husks. *Waste Management and Research*, **32**(4), 331–339. <https://doi.org/10.1177/0734242X14525822>
27. Song, W. & Guo, M. (2012) Quality variations of poultry litter biochar generated at different pyrolysis temperatures. *Journal of Analytical and Applied Pyrolysis*, **94**, 138–145. <https://doi.org/10.1016/j.jaap.2011.11.018>
28. Boehm, H. (1994) Some aspects of the surface chemistry of carbon blacks and other carbons. *Pergamon*, **32**(5), 759–769.
29. Salame, I. I. & Bandosz, T. J. (2001) Surface chemistry of activated carbons: Combining the results of temperature-programmed desorption, Boehm, and potentiometric titrations. *Journal of Colloid and Interface Science*, **240**(1), 252–258. <https://doi.org/10.1006/jcis.2001.7596>
30. Fahmi, A. H., Samsuri, A. W., Jol, H. & Singh, D. (2018) Physical modification of biochar to expose the inner pores and their functional groups to enhance lead adsorption. *RSC Advances*, **8**(67), 38270–38280. <https://doi.org/10.1039/c8ra06867d>
31. Tomczyk, A., Sokołowska, Z. & Boguta, P. (2020) Biochar physicochemical properties: pyrolysis temperature and feedstock kind effects. *Reviews in Environmental Science and Biotechnology*, **19**(1), 191–215. <https://doi.org/10.1007/s11157-020-09523-3>
32. Ayawei, N., Ebelegi, A. N. & Wankasi, D. (2017) Modelling and Interpretation of Adsorption Isotherms. *Journal of Chemistry*, **11**. <https://doi.org/10.1155/2017/3039817>
33. Sewu, D. D., Boakye, P. & Woo, S. H. (2017) Highly efficient adsorption of cationic dye by biochar produced with Korean cabbage waste. *Bioresource Technology*, **224**, 206–213. <https://doi.org/10.1016/j.biortech.2016.11.009>
34. Rebitanim, N. Z., Ghani, W. A. W. A. K., Mahmoud, D. K., Rebitanim, N. A. & Mohd Salleh, M. A. (2012) Adsorption Capacity of Raw Empty Fruit Bunch Biomass onto Methylene Blue Dye in Aqueous Solution. *Journal of Purity, Utility*

- Reaction and Environment*, **1**(February 2016), 45–60.
35. Ahmed, M. B., Zhou, J. L., Ngo, H. H., Guo, W. & Chen, M. (2016) Progress in the preparation and application of modified biochar for improved contaminant removal from water and wastewater. *Bioresource Technology*, **214** (May), 836–851. <https://doi.org/10.1016/j.biortech.2016.05.057>
  36. Hadjittofi, L., Prodromou, M. & Pashalidis, I. (2014) Activated biochar derived from cactus fibres - Preparation, characterization and application on Cu (II) removal from aqueous solutions. *Bioresource Technology*, **159**, 460–464. <https://doi.org/10.1016/j.biortech.2014.03.073>
  37. Qian, K., Kumar, A., Patil, K., Bellmer, D., Wang, D., Yuan, W. & Huhnke, R. L. (2013) Effects of biomass feedstocks and gasification conditions on the physiochemical properties of char. *Energies*, **6**(8), 3972–3986. <https://doi.org/10.3390/en6083972>
  38. Sizmur, T., Fresno, T., Akgül, G., Frost, H., Moreno, E. & Jiménez, (2017) Biochar modification to enhance sorption of inorganics from water. *Bioresource Technology*, **246**, 34–47. <https://doi.org/10.1016/j.biortech.2017.07.082>
  39. Saleh, S., Kamarudin, K. B., Ghani, W. A. W. A. K. & Kheang, L. S. (2016) Removal of Organic Contaminant from Aqueous Solution Using Magnetic Biochar. *Procedia Engineering*, **148**, 228–235. <https://doi.org/10.1016/j.proeng.2016.06.590>
  40. Peng, H., Gao, P., Chu, G., Pan, B., Peng, J. & Xing, B. (2017) Enhanced adsorption of Cu(II) and Cd(II) by phosphoric acid-modified biochars. *Environmental Pollution*, **229**, 846–853. <https://doi.org/10.1016/j.envpol.2017.07.004>
  41. Zhang, W., Li, H., Kan, X., Dong, L., Yan, H., Jiang, Z., Yang, H., Li, A. & Cheng, R. (2012) Adsorption of anionic dyes from aqueous solutions using chemically modified straw. *Bioresource Technology*, **117**, 40–47. <https://doi.org/10.1016/j.biortech.2012.04.064>
  42. Zhu, Y., Yi, B., Yuan, Q., Wu, Y., Wang, M. & Yan, S. (2018) Removal of methylene blue from aqueous solution by cattle manure-derived low temperature biochar. *RSC Advances*, **8**(36), 19917–19929. <https://doi.org/10.1039/c8ra03018a>
  43. Thoe, J., Surugau, N. & Chong, H. (2019) Application of Oil Palm Empty Fruit Bunch as Adsorbent: A Review. *Transactions on Science and Technology*, **6**(1), 9–26.
  44. Mohan, D., Sarswat, A., Ok, Y. S. & Pittman, C. U. (2014) Organic and inorganic contaminants removal from water with biochar, a renewable, low cost and sustainable adsorbent--a critical review. *Bioresource Technology*, **160**, 191–202. <https://doi.org/10.1016/j.biortech.2014.01.120>
  45. Vithanage, M., Rajapaksha, A. U. Pamali, Zhang, M., Thiele-Bruhn, S., Lee, S. S. Oo, & Ok, Y. S. ik. (2015) Acid-activated biochar increased sulfamethazine retention in soils. *Environmental Science and Pollution Research International*, **22**(3), 2175–2186. <https://doi.org/10.1007/s11356-014-3434-2>
  46. Sun, Y., Gao, B., Yao, Y., Fang, J., Zhang, M., Zhou, Y., Chen, H. & Yang, L. (2014) Effects of feedstock type, production method, and pyrolysis temperature on biochar and hydrochar properties. *Chemical Engineering Journal*, **240**, 574–578. <https://doi.org/10.1016/j.cej.2013.10.081>
  47. Ma, Y., Liu, W. J., Zhang, N., Li, Y. S., Jiang, H. & Sheng, G. P. (2014) Polyethylenimine modified biochar adsorbent for hexavalent chromium removal from the aqueous solution. *Bioresource Technology*, **169**, 403–408. <https://doi.org/10.1016/j.biortech.2014.07.014>
  48. Djilani, C., Zaghdoudi, R., Djazi, F. & Boucekima, B. (2015) Journal of the Taiwan Institute of Chemical Engineers Adsorption of dyes on activated carbon prepared from apricot stones and commercial activated carbon. **53**, 112–121. <https://doi.org/10.1016/j.jtice.2015.02.025>
  49. Kavitha, B., Jothimani, P. & Rajannan, G. (2013) Empty Fruit Bunch- a Potential Organic Manure for Agriculture. *International Journal of Science, Environment and Technology*, **2**(5), 930–937.
  50. Komnitsas, K. A. & Zaharaki, D. (2016) Morphology of Modified Biochar and Its Potential for Phenol Removal from Aqueous Solutions. *Frontiers in Environmental Science*, **4** (April), 1–11. <https://doi.org/10.3389/fenvs.2016.00026>
  51. Godwin, P. M., Pan, Y., Xiao, H. & Afzal, M. T. (2019) Progress in Preparation and Application of Modified Biochar for Improving Heavy Metal Ion Removal From Wastewater. *Journal of Bioresources and Bioproducts*, **4**(1), 31–42. <https://doi.org/10.21967/jbb.v4i1.180>
  52. Wong, S., Tumari, H. H., Ngadi, N., Mohamed, N. B., Hassan, O., Mat, R., Aishah, N. & Amin, S. (2019) Adsorption of anionic dyes on spent tea

- leaves modified with polyethyleneimine ( PEI-STL ). *Journal of Cleaner Production*, **206**, 394–406.
53. Wong, Y. C., Szeto, Y. S., Cheung, W. H. & McKay, G. (2004) Adsorption of acid dyes on chitosan - Equilibrium isotherm analyses. *Process Biochemistry*, **39(6)**, 695–704. [https://doi.org/10.1016/S0032-9592\(03\)00152-3](https://doi.org/10.1016/S0032-9592(03)00152-3)
  54. Park, J. H., Wang, J. J., Meng, Y., Wei, Z., DeLaune, R. D. & Seo, D. C. (2019) Adsorption/desorption behavior of cationic and anionic dyes by biochars prepared at normal and high pyrolysis temperatures. *Colloids and Surfaces A: Physicochemical and Engineering Aspects*, **572** (February), 274–282. <https://doi.org/10.1016/j.colsurfa.2019.04.029>
  55. Saad, S. a, Daud, S., Kasim, F. H. & Saleh, M. N. (2007) Methylene blue removal from simulated wastewater by adsorption using treated oil palm empty fruit bunch. *ICoSM2007 Paper, May*, 293–296.
  56. Valix, M., Cheung, W. H. & McKay, G. (2004) Preparation of activated carbon using low temperature carbonisation and physical activation of high ash raw bagasse for acid dye adsorption. *Chemosphere*, **56(5)**, 493–501. <https://doi.org/10.1016/j.chemosphere.2004.04.004>
  57. Çağlar, E., Donar, Y. O., Sinag, A., Biro Gul, I., Bilge, S., Aydinçak, K. & Pliekhov, O. (2018) Adsorption of anionic and cationic dyes on biochars, produced by hydrothermal carbonization of waste biomass: Effect of surface functionalization and ionic strength. *Turkish Journal of Chemistry*, **42(1)**, 86–99. <https://doi.org/10.3906/kim-1704-12>
  58. He, C. & Hu, X. (2011) Anionic dye adsorption on chemically modified ordered mesoporous carbons. *Industrial & Engineering Chemistry Research*, **50**, 14070–14083. <https://doi.org/10.1021/ie201469p>
  59. Gong, R., Sun, Y., Chen, J., Liu, H. & Yang, C. (2005) Effect of chemical modification on dye adsorption capacity of peanut hull. *Dyes and Pigments*, **67(3)**, 175–181. <https://doi.org/10.1016/j.dyepig.2004.12.003>
  60. Wong, S., Ghafar, N. A., Ngadi, N., Razmi, F. A., Inuwa, I. M., Mat, R. & Amin, N. A. S. (2020) Effective removal of anionic textile dyes using adsorbent synthesized from coffee waste. *Scientific Reports*, **10(1)**, 1–13. <https://doi.org/10.1038/s41598-020-60021-6>